SCIENTIFIC REPORTS

OPEN

SUBJECT AREAS:
IMMUNOLOGY
CELL DEATH AND IMMUNE RESPONSE

Received
8 November 2013

Accepted
16 June 2014

Published
25 July 2014

Correspondence and requests for materials should be addressed to S.M. (shibnath1@yahoo.co.in)

# Ameliorating ER-stress attenuates *Aeromonas hydrophila*-induced mitochondrial dysfunctioning and caspase mediated HKM apoptosis in *Clarias batrachus*

Chaitali Banerjee[1], Ambika Singh[2], Taposh Kumar Das[3], Rajagopal Raman[2], Anju Shrivastava[4] & Shibnath Mazumder[1]

[1]Immunobiology Laboratory, Department of Zoology, University of Delhi, Delhi 110 007, India, [2]Gut Biology Laboratory, Department of Zoology, University of Delhi, Delhi 110 007, India, [3]Department of Anatomy, All India Institute of Medical Sciences, Delhi 110 029, India, [4]Cell Signalling and Molecular Immunology Laboratory, Department of Zoology, University of Delhi, Delhi 110 007, India.

**Endoplasmic reticulum (ER)-stress and unfolding protein response (UPR) has not been implied in *Aeromonas hydrophila*-pathogenicity. We report increased expression of the ER-stress markers: CHOP, BiP and phospho-eIF2α in *A. hydrophila*-infected headkidney macrophages (HKM) in *Clarias batrachus*. Pre-treatment with ER-stress inhibitor, 4-PBA alleviated ER-stress and HKM apoptosis suggesting ER-UPR critical for the process. The ER-$Ca^{2+}$ released *via* inositol-triphosphate and ryanodine receptors induced calpain-2 mediated superoxide ion generation and consequent NF-κB activation. Inhibiting NF-κB activation attenuated NO production suggesting the pro-apoptotic role of NF-κB on HKM pathology. Calpain-2 activated caspase-12 to intensify the apoptotic cascade through mitochondrial-membrane potential ($\psi_m$) dissipation and caspase-9 activation. Altered mitochondrial ultra-structure consequent to ER-$Ca^{2+}$ uptake *via* uniporters reduced $\psi_m$ and released cytochrome C. Nitric oxide induced the cGMP/PKG-dependent activation of caspase-8 and truncated-Bid formation. Both the caspases converge onto caspase-3 to execute HKM apoptosis. These findings offer a possible molecular explanation for *A. hydrophila* pathogenicity.**

*Aeromonas hydrophila* Gram-negative bacteria, is the predominant cause of ulcerative disease syndrome (UDS) in fish[1]. It also causes soft tissue infections, gastroenteritis and septicaemia in humans[2]. However, *A. hydrophila*-induced pathogenicity is not well understood. Macrophages are essential for innate immune responses against *A. hydrophila* and apoptosis has been extensively implicated in macrophage-*A. hydrophila* interactions[3,4]. However, it is difficult to predict whether the outcomes are to the advantage of the host or the pathogen[5].

*A. hydrophila*-induced macrophage apoptosis is executed by an intracellular proteolytic cascade of caspases, where initiator caspases are triggered by a range of intracellular signalling molecules to accomplish programmed demolition of cell through caspase-3 activation[3,4,6]. As an early initiator of the process, the role of calcium ($Ca^{2+}$) is foremost[7]. Among other molecules that initiate *A. hydrophila*-induced apoptosis, reactive oxygen species (ROS) is important. The NF-κB pathway is induced in response to ROS accumulation and has been implicated as both pro- and anti-survival under different conditions[8]. Among the different pro-apoptotic molecules which are up-regulated by NF-κB, inducible nitric oxide synthase (*i*NOS) mediated nitric oxide (NO) production is fairly well-studied. NO acts on a number of target enzymes and proteins and activation of cGMP-dependent PKG is one[9].

The sub-cellular organelle ER, a major intracellular $Ca^{2+}$ source, is the site for appropriate protein folding leading to production of functionally mature proteins and is emerging as crucial player in apoptosis induction[10]. Consequent to $[ER]_{Ca}{}^{2+}$ depletion, increased accumulation of mis-folded proteins take place in the ER lumen causing ER-stress. ER-stress is sensed by three membrane located sensors: RNA-dependent protein kinase-like

ER kinase (PERK), activating transcription factor 6 (ATF6) and inositol-requiring ER-to-nucleus signal kinase 1 (IRE1). To alleviate ER-stress, cells initiate the UPR programme characterized by the phosphorylation of eukaryotic translation initiation factor 2α (eIF2α), expression of glucose regulated protein 78 (GRP78/BiP) and CCAAT/enhancer-binding protein-homologous protein (CHOP)[11]. The expression of CHOP, BiP and phospho-eIF2α are thus considered as markers for ER-stress.

Stress initiates the depletion of $[ER]_{Ca}^{2+}$ through the inositol 1,4,5-triphosphate receptors (IP3R) and ryanodine receptor (RyR) present on ER. It activates calpain in the cytosol, which cleaves procaspase-12 to mature caspase-12 in the ER[12]. Activated caspase-12 further intensifies the apoptotic cascade through the activation of caspase-9 and caspase-3. This pathway is known as the intrinsic pathway and mitochondrial permeabilization is crucial in it. Bid, released *via* caspase-8 (extrinsic pathway) plays a key role on mitochondrial permeabilization and caspase-9 activity[13]. It has recently been hypothesized that under stress the ER and mitochondria come in close proximity and the $[ER]_{Ca}^{2+}$ is taken up by the mitochondrial uniporters (MUP) thereby dissipating $\psi_m$ and opening the mitochondrial permeability transition pores (MPTP), triggering apoptosis[14]. Importantly, though ER-stress has been fairly well-reported in mammals it is not well-characterised in the fish system[15].

Fish are the natural host of *A. hydrophila*[1]. They occupy a key position in the course of evolution being the earliest class of vertebrates possessing both innate and adaptive immunity. The fish innate immune system, akin to that in mammals, serves as the first line of defence against pathogens[16]. Unlike higher vertebrates, HK is the principal immune organ in fish and even regulates the neuro-immuno-endocrine axis[17]. The HKM play critical role in defence against invading pathogens and is an alternative model to study *A. hydrophila*-pathogenicity at cellular level[18].

*A. hydrophila* induces apoptosis in fish[4,19] but the exact mechanisms are not clearly elucidated. We demonstrated *A. hydrophila*-induced apoptosis to be caspase-3 mediated and $Ca^{2+}$ and its dependent neutral protease calpain-2, critical for initiating the death program[4]. However the potential role of other signalling molecules in *A. hydrophila*-induced HKM apoptosis is yet to be investigated.

We therefore addressed the role of ER-stress on *A. hydrophila*-induced HKM apoptosis. We suggest ER-stress activates the calpain-2-caspase-12-superoxide ion-NF-κB axis causing mitochondrial dysfunction in *A. hydrophila*-infected HKM.

## Results

***A. hydrophila*-induced ER-stress is critical for initiating HKM apoptosis.** The upregulation of ER stress proteins is a marker for altered ER homeostasis and subsequently apoptosis[20]. The expressions of CHOP, BiP and eIF2α phosphorylation were thus studied in *A. hydrophila*-infected HKM by confocal microscopy. Our results suggested that BiP expression significantly increased following 1 h post-infection (p.i.) (≈6.0 fold) which gradually decreased to 1.6 fold, 24 h p.i. (Fig. 1a and Supplementary Fig. 1a). Nonetheless, CHOP expression was increased throughout the course of infection (2.3–2.6 fold, Fig. 1a and Supplementary Fig. 1a). Confocal microscopy also indicated enhanced phospho-eIF2α expression in infected HKM (2.3–3.0 fold, Fig. 1a and Supplementary Fig. 1a). No significant change was noted in the total-eIF2α levels during infection (data not shown). To correlate ER-stress to *A. hydrophila*-induced pathogenicity, the HKM were pre-treated with the general ER-stress inhibitor, 4-PBA and the expression of CHOP, BiP, phospho-eIF2α and ensuing HKM apoptosis studied. We observed marked inhibition in CHOP, BiP and phospho-eIF2α expression in infected HKM (Fig. 1b and Supplementary Fig. 1b, 1c, 1d). Besides, 4-PBA pre-treatment also attenuated *A. hydrophila*-induced HKM apoptosis (Supplementary Fig. 2). Together these results implicate ER-stress-mediated CHOP-BiP-phospho-eIF2α spree is critical in *A. hydrophila*-induced HKM apoptosis.

Activation of ER-stress proteins is a downstream consequence of $[ER]_{Ca}^{2+}$ depletion which in turn is implicated in apoptosis[20]. Hence, as next step, we studied the role of $[ER]_{Ca}^{2+}$ on HKM apoptosis. We observed that Xes and Dant, inhibitors to IP3R and RyR respectively inhibited the expression of CHOP, BiP and phospho-eIF2α (Fig. 1b and Supplementary Fig. 1b, 1c, 1d) and attenuated HKM apoptosis (Supplementary Fig. 2), thus implicating $[ER]_{Ca}^{2+}$ depletion on initiating ER-stress protein activation in *A. hydrophila*-infected HKM.

**Calpain-2 augments ER-stress by activating caspase-12 in infected HKM.** We had earlier reported calpain-2 critical for *A. hydrophila*-mediated HKM apoptosis[4]. To document a link between ER stress and calpain-2 activation, the HKM were pre-treated with 4-PBA and calpain-2 activity checked by immunoblotting. It is evident from Fig. 1c, that alleviation of ER-stress down-regulated calpain-2 expression in *A. hydrophila*-infected HKM. However, the converse was not true as calpain-2 inhibitor failed to impact ER-stress protein expression in infected HKM (data not shown). Hence, we suggest ER-stress is critical for activating calpain-2 in *A. hydrophila*-infected HKM.

Calpain-2 has been implicated in the activation of caspase-12, an endogenous marker for ER-stress[12]. Confocal microscopy recommended significant increase in caspase-12 activity in *A. hydrophila*-infected HKM (Fig. 1d). Pre-treatment with the caspase-12 inhibitor, Z-ATAD-FMK inhibited caspase-12 activation (Fig. 1d) and attenuated *A. hydrophila*-induced HKM apoptosis (Supplementary Fig. 2). Next, the role of calpain-2 on caspase-12 activation was investigated. HKM were pre-treated with calpain-2*i* and we noted that caspase-12 levels were significantly reduced in the infected HKM (Fig. 1d and Supplementary Fig. 3a) suggesting ER-stress induced by *A. hydrophila* to activate calpain-2 initiating downstream caspase-12 activity in HKM.

***A. hydrophila*-induced superoxide ion generation is calpain-2 dependent.** Superoxide ion production plays an important role in microbial pathogenicity[21]. We observed significant amount of superoxide ion production at 1 h p.i. which attained peak at 4 h p.i., thereafter the levels gradually declined reaching basal level at 24 h p.i. (Fig. 2a). We suspected NADPH Oxidase to be involved in the process and for that the HKM were pre-treated with NADPH Oxidase inhibitors-Apo and DPI, prior to studying superoxide ion production. The 4 h interval was selected as maximum superoxide ion production was recorded during this time point. It is evident from Fig. 2b that pre-treatment with Apo and DPI led to significant decline in *A. hydrophila*-induced superoxide ion levels. To corroborate our observation, we further studied membrane translocation of $p47^{phox}$, which is an index of NADPH Oxidase activation[22]. Immunoblotting suggested marked increase in $p47^{phox}$ expression in the membrane fraction of *A. hydrophila*-infected HKM which was inhibited in presence of Apo or DPI. The cytosolic fraction of the same samples was probed with anti-β-actin to confirm for equal loading (Fig. 2c).

The next aim was establishing the role of superoxide ion on HKM apoptosis. The HKM were pre-treated with Apo and DPI and apoptosis studied at 24 h p.i. We noted that both Apo and DPI significantly attenuated *A. hydrophila*-induced HKM apoptosis (Supplementary Fig. 2) suggesting superoxide ion critical for *A. hydrophila*-induced HKM pathology. On establishing the involvement of superoxide ion on *A. hydrophila*-induced HKM pathology we sought to study the cross-talk between calpain-2*i* activation and superoxide ion generation. We observed that attenuating calpain-2 activation inhibited $p47^{phox}$ membrane translocation and superoxide ion generation in the infected HKM (Fig. 2b and 2c). On the contrary, pre-treatment with Apo and DPI failed to impact calpain-2 activation (Fig. 1c), suggesting superoxide ion generation is downstream to

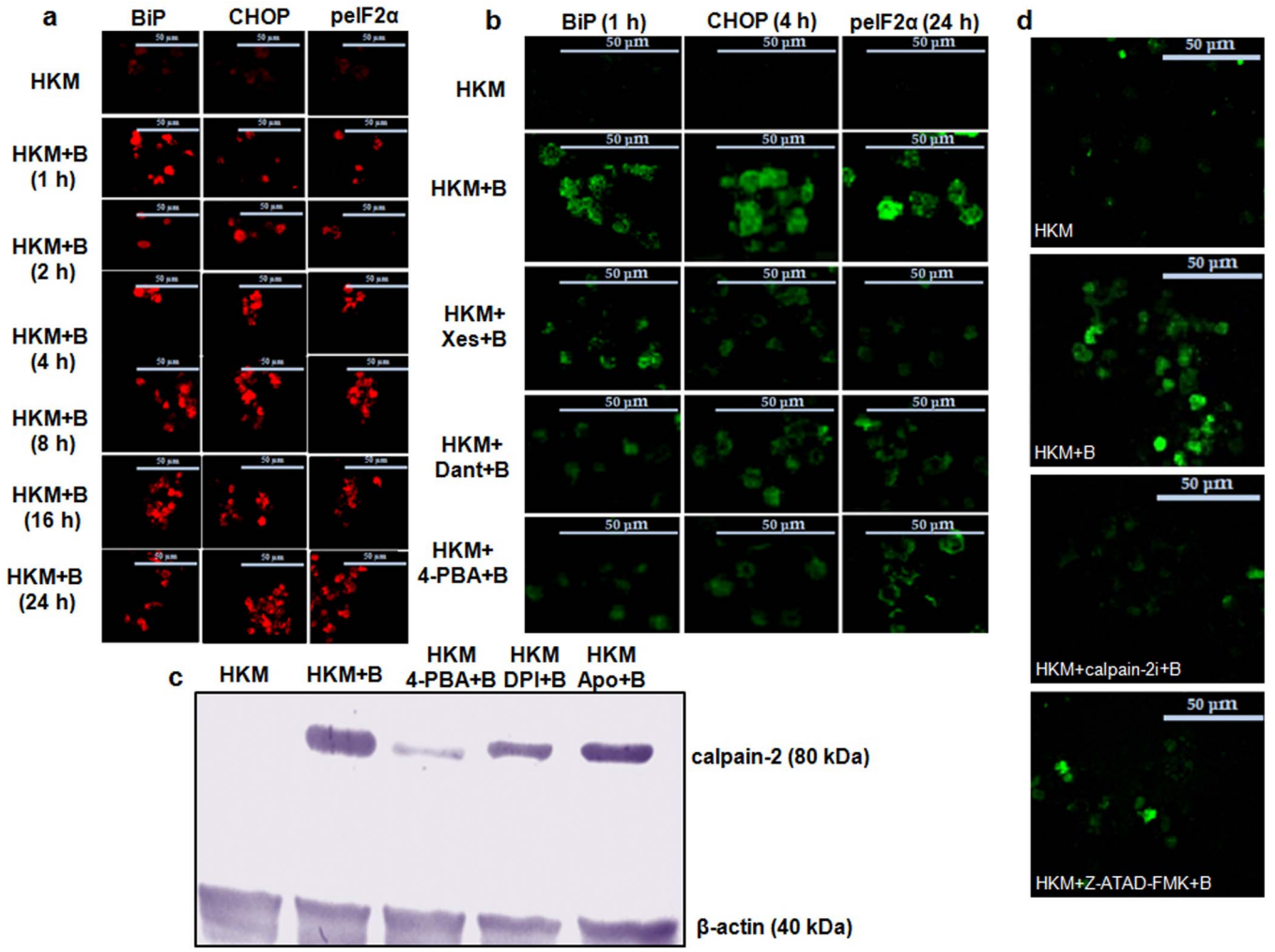


**Figure 1** | ***A. hydrophila*-induced ER-stress triggers calpain-2 mediated caspase-12 activation in HKM.** (a) HKM were infected with *A. hydrophila* and at indicated time p.i. BiP (left panel), CHOP (middle panel) and p-eIF2α (right panel) expression studied by immunofluorescence. TRITC-conjugated secondary antibody used for red fluorescence. (b) HKM were pre-treated separately with Xes, Dant and 4-PBA and expression of BiP (left panel), CHOP (middle panel) and p-eIF2α (right panel) studied by immunofluorescence at 1 h, 4 h and 24 h p.i. FITC-conjugated secondary antibody used for green fluorescence. (c) Representative western blot for calpain-2 expression in lysates of HKM pre-treated separately with 4-PBA, DPI and Apo at 24 h p.i. β-actin served as the loading control. (d) HKM were pre-treated separately with calpain-2*i* and Z-ATAD-FMK and at 24 h p.i. caspase-12 activity checked. The images are representative of three independent experiments and observed under confocal microscope (×40). HKM, uninfected control; HKM + B, HKM infected with *A. hydrophila*; HKM + 4-PBA + B, HKM pre-treated with 4-PBA for 1 h before *A. hydrophila*-infection; HKM + Xes + B, HKM pre-treated with xestospongin C for 1 h before *A. hydrophila*-infection; HKM + Dant + B, HKM pre-treated with dantrolene for 1 h before *A. hydrophila*-infection; HKM + Z-ATAD-FMK + B, HKM pre-treated with Z-ATAD-FMK for 1 h before *A. hydrophila*-infection; HKM + calpain-2*i* + B, HKM pre-treated with calpain-2*i* for 1 h before *A. hydrophila*-infection; HKM + Apo + B, HKM pre-treated with Apo for 1 h before *A. hydrophila*-infection; HKM + DPI + B, HKM pre-treated with DPI for 2 h before *A. hydrophila*-infection. 4-PBA, ER-stress protein inhibitor; Xes, IP3R inhibitor; Dant, RyR inhibitor; Z-ATAD-FMK, caspase-12 inhibitor; calpain-2*i*, calpain-2 inhibitor; Apo and DPI, NADPH Oxidase inhibitor.

calpain-2 activation. To conclude, these results suggest calpain-2 induces NADPH Oxidase mediated superoxide ion generation in *A. hydrophila*-infected HKM.

**NF-κB is pro-apoptotic in *A. hydrophila*-infected HKM.** NF-κB activation is redox-regulated[23] and implicated in microbial-pathogenicity[8]. In the present study we selected p65/RelA phosphorylation as an index for NF-κB activation[24]. At the onset, p65-phosphorylation was studied in the HKM at different time intervals using specific EIA kit. We observed time dependent increase in p65-phosphorylation with maximum changes recorded at 16 h p.i. in infected HKM. The levels of total-p65 remained unaltered during the entire time course (Fig. 3a). Following activation, NF-κB translocates from the cytoplasm to nucleus mediating its effects. We studied nuclear translocation of NF-κB using phospho-p65 antibodies and immunofluorescence studies demonstrated nuclear localization of phospho-p65 suggesting sustained NF-κB activation in the infected HKM (Fig. 3c). The next step was correlating this important molecular event in the pathology of *A. hydrophila*. Hence, HKM were pre-treated with the NF-κB inhibitor, NF-κB*i* and apoptosis studied. We report that pre-treatment with NF-κB*i* inhibited phosphorylation (Fig. 3b) and nuclear translocation of p65 (Fig. 3c) besides attenuating HKM apoptosis (Supplementary Fig. 2). Based on these results we suggest NF-κB plays pro-apoptotic role in *A. hydrophila*-induced HKM apoptosis.

We correlated NF-κB activation with superoxide ion generation. From our results it is evident that NF-κB activity is superoxide ion-dependent and pre-treatment with Apo and DPI inhibited p65-phosphorylation (Fig. 3b) and nuclear translocation (Fig. 3c). Overall, we propose that superoxide ion triggers NF-κB in *A. hydrophila*-infected HKM leading to the activation of downstream pro-apoptotic genes.

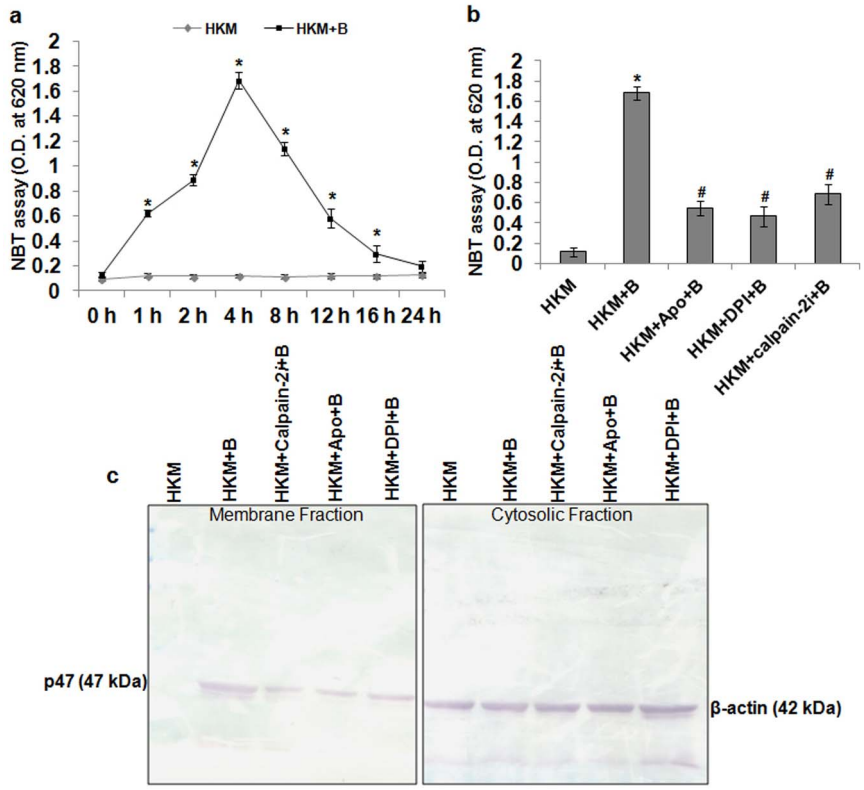


**Figure 2 | Calpain-2 induces NADPH Oxidase mediated superoxide ion production *in A. hydrophila*-infected HKM.** (a) HKM were infected with *A. hydrophila* and at indicated time p.i. superoxide ion production measured by NBT assay. Statistically significant amount of superoxide ion was detected at 1 h p.i. and it continued till 16 h p.i. (*$P < 0.001$/F = 341.6). (b) HKM were pre-treated separately with Apo, DPI and calpain-2*i* and superoxide ion production measured at 4 h p.i. Pre-treatment with the inhibitors significantly lowered superoxide ion production in the infected-HKM (*, $^{\#}P < 0.001$/F = 125.4). (c) HKM were pre-treated separately with Apo, DPI and calpain-2*i* and at 4 h p.i. $p47^{phox}$ membrane translocation studied by immunoblotting. The cytosolic fraction was probed with β-actin to confirm for equal loading. **P* *vs* HKM; $^{\#}P$ *vs* HKM + B. Vertical bars represent mean ± SE (n = 6). HKM, uninfected control; HKM + B, HKM infected with *A. hydrophila*; HKM + Apo + B, HKM pre-treated with Apo for 1 h before *A. hydrophila*-infection; HKM + DPI + B, HKM pre-treated with DPI for 2 h before *A. hydrophila*-infection; HKM + calpain-2*i* + B, HKM pre-treated with calpain-2*i* for 1 h before *A. hydrophila*-infection. Apo and DPI, NADPH Oxidase inhibitor; calpain-2*i*, calpain-2 inhibitor.

**NF-κB induces pro-apoptotic NO release in infected HKM.** Though, *A. hydrophila*-induced NO production is reported in fish[25] the molecular mechanisms is not well understood. We first measured NO production and noted time dependent increase in NO levels with the maximum production recorded 24 h p.i. in the infected HKM (Fig. 4a). Next we studied *i*NOS activity and immunofluorescence results suggested significant *i*NOS activity in infected HKM that underwent marked reduction in presence of the specific *i*NOS inhibitor, L-Nil (Fig. 4b and Supplementary Fig. 3b). Pre-treatment with L-Nil also interfered with NO production (Fig. 4c) and attenuated HKM apoptosis (Supplementary Fig. 2) suggesting the pro-apoptotic role of *i*NOS-induced NO in *A. hydrophila*-pathogenicity. To investigate whether superoxide ion-NF-κB axis influenced *i*NOS activity, the HKM were pre-treated with NF-κB*i* and *i*NOS expression and NO production studied. We noted that pre-treatment with NF-κB*i* significantly attenuated *i*NOS expression (Fig. 4b) and NO production (Fig. 4c). The converse however was not observed as L-Nil failed to lower phospho-p65 levels in infected HKM (Fig. 3b). Based on our observations we suggest NF-κB mediates pro-apoptotic effect *via* activation of *i*NOS in *A. hydrophila*-infected HKM and superoxide ion primal in initiating the process.

***A. hydrophila*-induced caspase-8 activation is cGMP-PKG dependent.** We had earlier demonstrated *A. hydrophila*-induced HKM apoptosis to be caspase-3 mediated[4]. Here, we investigated the role of caspase-8 on caspase-3 activation. Using specific assay kits, we observed increased caspase-8 activity in infected HKM, which was inhibited in the presence of specific caspase-8 inhibitor, Z-IETD-FMK (Fig. 4d). This encouraged us to study the presence of t-Bid, an indicator of caspase-8 activation by immunoblotting. We observed Bid fragmentation in infected HKM that was inhibited in the presence of Z-IETD-FMK (Fig. 4e). Besides, Z-IETD-FMK also attenuated HKM apoptosis by inhibiting caspase-3 activation (Supplementary Fig. 2). Our results suggest caspase-8 initiates caspase-3 mediated apoptosis of *A. hydrophila*-infected HKM.

The next aim was correlating the upstream molecular events leading to caspase-8 activation. cGMP has been reported to be pro-apoptotic under different conditions of stress and acts downstream of NO[9]. We first measured cGMP levels at 24 h p.i. because at this time point we recorded maximum NO production in infected HKM. Our results clearly indicate that the levels of cGMP were significantly elevated in the infected HKM and pre-treatment with cGMP inhibitor, LY83583 reduced cGMP levels (Fig. 4f) and rescued the cells from apoptosis (Supplementary Fig. 2). The cell-permeable cGMP analogue (8-Br-cGMP) also elevated intracellular cGMP level (Fig. 4f) and induced HKM apoptosis (Supplementary Fig. 2). Further, pre-treatment with L-Nil also inhibited *A. hydrophila*-induced cGMP production in HKM (Fig. 4f). These results suggest NO-dependent cGMP is a critical factor in the initiation of *A. hydrophila*-induced HKM apoptosis.

PKG is an important intermediate in transmitting NO-induced cGMP signals[26]. To establish the role of cGMP-PKG axis, HKM were pre-treated with the PKG inhibitor, KT5823 and caspase-8 activity

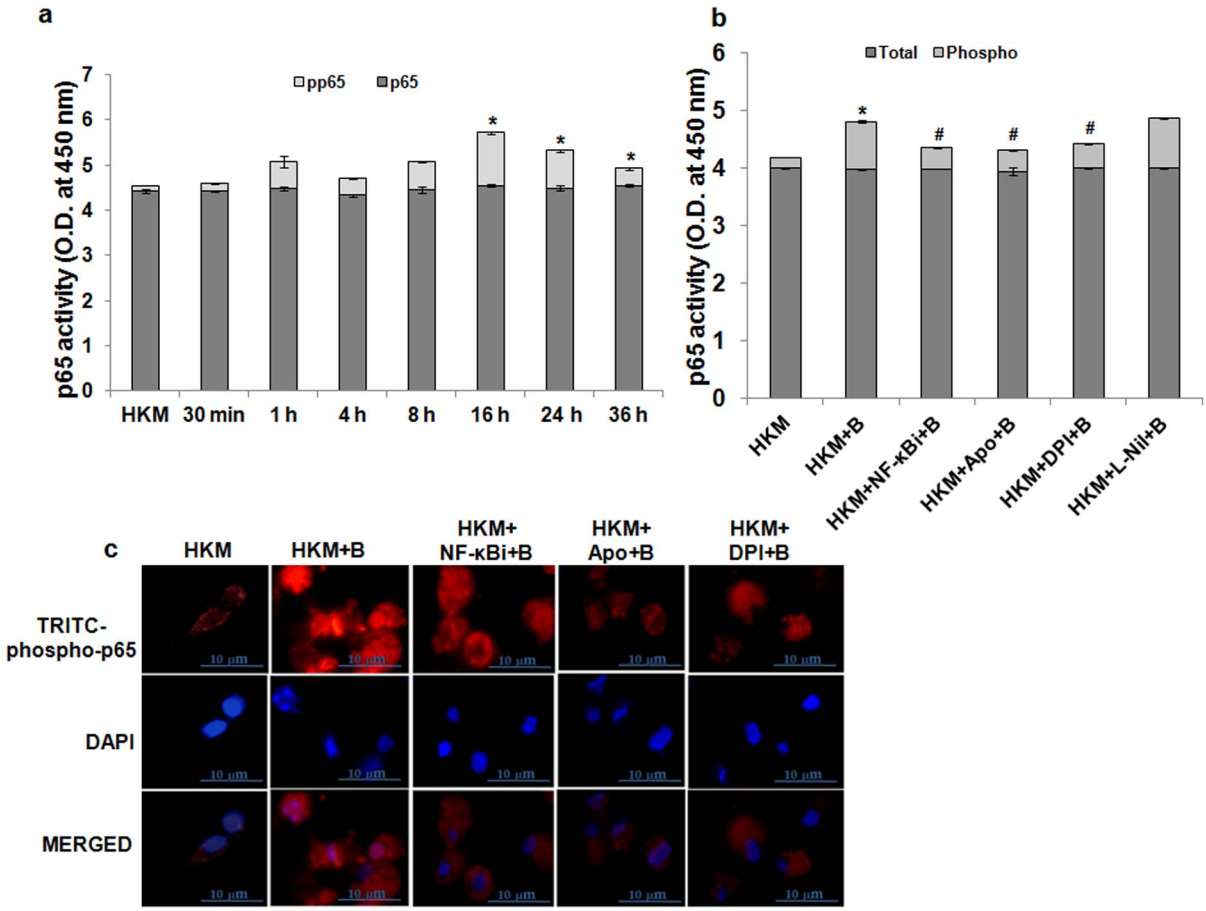


**Figure 3 | NF-κB activation is pro-apoptotic in *A. hydrophila*-infected HKM.** (a) HKM were infected with *A. hydrophila* and at indicated time p.i. changes in total and phosphorylated NF-κB-p65 measured in lysates using EIA kits. No significant change in total NF-κB values were noted ($P = 0.9826/F = 0.1785$). However, phosphorylated NF-κB levels increased significantly at 16 h p.i. and beyond (*$P = 0.0028/F = 9.157$). (b) HKM were pre-treated separately with NF-κB*i*, Apo, DPI and L-Nil and at 24 h p.i. changes in total and phosphorylated NF-κB-p65 measured in lysates using EIA kits. Statistical significance was apparent in infected samples relative to uninfected HKM for phosphorylated NF-κB-p65 levels. Also pre-treatment with the inhibitors separately significantly lowered phosphorylated NF-κB-p65 levels relative to infected sets (*, $^{\#}P < 0.001/F = 480.5$). However, no significant change was observed for total NF-κB-p65 levels in different groups ($P = 0.583/F = 4.080$). (c) HKM were pre-treated separately with NF-κB*i*, Apo and DPI and at 24 h p.i. nuclear translocation of phosphorylated NF-κB-p65 studied by immunofluorescence (×100). TRITC-conjugated secondary antibody used for red fluorescence and nuclear staining was done with DAPI. The images are representative of three independent experiments. *$P$ *vs* HKM; $^{\#}P$ *vs* HKM + B. Vertical bars represent mean ± SE (n = 6). HKM, uninfected control; HKM + B, HKM infected with *A. hydrophila*; HKM + Apo + B, HKM pre-treated with Apo for 1 h before *A. hydrophila*-infection; HKM + DPI + B, HKM pre-treated with DPI for 2 h before *A. hydrophila*-infection; HKM + NF-κB*i* + B, HKM pre-treated with NF-κB*i* for 1 h before *A. hydrophila*-infection; HKM + L-Nil + B, HKM pre-treated with L-Nil for 1 h before *A. hydrophila*-infection. NF-κB*i*, NF-κB activation inhibitor; Apo and DPI, NADPH Oxidase inhibitor; L-Nil, *i*NOS-specific inhibitor.

and apoptosis studied. We observed that KT5823 pre-treatment inhibited caspase-8 activity (Fig. 4d) and attenuated HKM apoptosis (Supplementary Fig. 2). Besides, LY83583 also inhibited caspase-8 activation in the infected HKM (Fig. 4d). Taken together, the results suggest caspase-8 activation to be NO-initiated cGMP-PKG dependent in *A. hydrophila*-infected HKM.

**ER-mitochondria cross-talk is a critical event in *A. hydrophila*-infected HKM.** Alterations in mitochondrial-$Ca^{2+}$ has been reported important for microbial pathogenicity[27]. To look into this we measured mitochondrial-$Ca^{2+}$ in *A. hydrophila*-infected HKM. Using a combination of Rhod-2 and mitotracker green we observed that mitochondrial-$Ca^{2+}$ uptake occurred within 30 mins of *A. hydrophila*-infection that reached its peak at 1 h p.i. and thereafter the levels started declining reaching the basal level 4 h p.i. (Fig. 5a and Supplementary Fig. 3c). Ruthenium Red (RR), a MUP-inhibitor blocks mitochondrial-$Ca^{2+}$ uptake[28]. We observed that pre-treatment with RR significantly decreased Rhod-2 fluorescence intensity proving MUP-mediated $Ca^{2+}$ uptake in the infected HKM (Fig. 5b and Supplementary Fig. 3d).

When we asked the source of mitochondrial-$Ca^{2+}$, ER appeared attractive. Hence, HKM were treated with Xes or Dant prior to *A. hydrophila*-infection and changes in mitochondrial-$Ca^{2+}$ levels studied. From Fig. 5b and Supplementary Fig. 3d, it is evident that Xes and Dant reduced mitochondrial-$Ca^{2+}$ load, thereby confirming our hypothesis. To check the probable mechanism of mitochondrial-$Ca^{2+}$ uptake we studied the interim relationship between ER and mitochondria. The *A. hydrophila*-infected HKM were observed under TEM at early (1 h) and late (24 h) stages of infection. We visualised a change in the sub-cellular arrangement at early stages of infection with the mitochondria in close apposition with ER. TEM analysis at 24 h p.i., revealed electron dense mitochondria to be docked onto the ER (Fig. 6a).To confirm the cross-talk between the two organelles we performed co-localization studies using the fluorescence probes, ER-tracker and mitotracker green. Our results confirmed that mitochondria co-localizes with ER which was more prominent in HKM collected at late stages of infection (Fig. 5c).

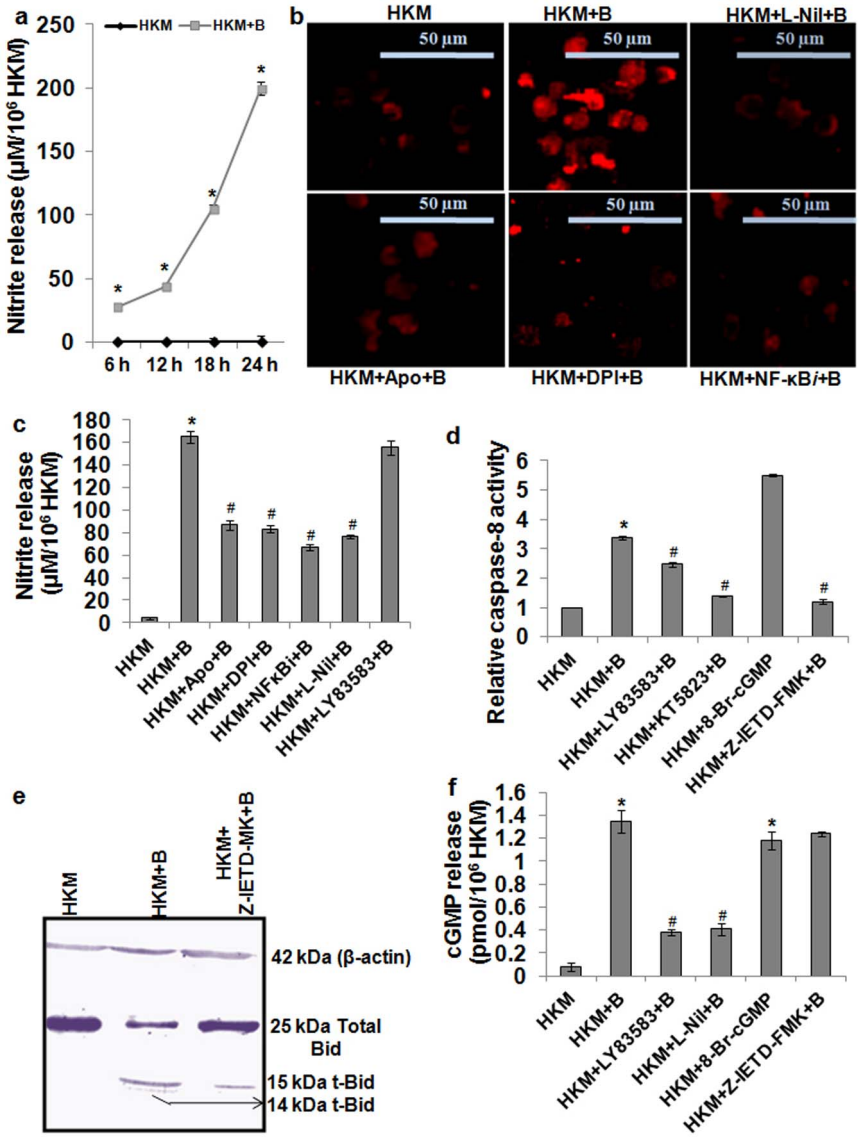


**Figure 4 | NO-cGMP/PKG activates caspase-8 in *A. hydrophila*-infected HKM.** (a) HKM were infected with *A. hydrophila* and NO release measured. Statistically significant amount of NO was detected at all time points (*$P < 0.001$/F = 399.8). (b) HKM were pre-treated separately with L-Nil, Apo, DPI and NF-κB*i* and *i*NOS expression checked at 24 h p.i. (c) HKM were pre-treated separately with Apo, DPI, NF-κB*i*, L-Nil and LY83583 and at 24 h p.i. NO release measured. Increase was significant in infected samples relative to uninfected HKM which significantly lowered following pre-incubation with inhibitors (*, #$P < 0.001$/F = 210.9). (d) HKM were pre-treated separately with LY83583, KT5823 and Z-IETD- and caspase-8 activity assayed 24 h p.i. 8-Br-cGMP set was not infected. Increase was significant in infected samples relative to uninfected HKM which significantly lowered following pre-incubation with inhibitors (*, #$P < 0.001$/F = 98.45). (e) Representative western blot for Bid/t-Bid in lysates of HKM pre-treated with Z-IETD-FMK at 24 h p.i. β-actin served as the loading control. (f) HKM were pre-treated separately with LY83583, L-Nil and Z-IETD-FMK and cGMP release checked in the cell lysates 24 h p.i. 8-Br-cGMP served as positive control. Increase was significant in infected samples relative to uninfected HKM which significantly lowered following pre-incubation with inhibitors (*, #$P < 0.001$/F = 47.37). *$P$ *vs* HKM; #$P$ *vs* HKM + B. Vertical bars represent mean ± SE (n = 6). The image represents best of three replicates. HKM, uninfected control; HKM + B, HKM infected with *A. hydrophila*; HKM + Apo + B, HKM pre-treated with Apo for 1 h before *A. hydrophila*-infection; HKM + DPI + B, HKM pre-treated with DPI for 2 h before *A. hydrophila*-infection; HKM + NF-κB*i* + B, HKM pre-treated with NF-κB*i* for 1 h before *A. hydrophila*-infection; HKM + L-Nil + B, HKM pre-treated with L-Nil for 1 h before *A. hydrophila*-infection; HKM + LY83583 + B, HKM pre-treated with LY83583 for 1 h before *A. hydrophila*-infection; HKM + Z-IETD-FMK + B, HKM pre-treated with Z-IETD-FMK for 1 h before *A. hydrophila*-infection; HKM + KT5823 + B, HKM pre-treated with KT5823 for 1 h before *A. hydrophila*-infection. L-Nil, *i*NOS-specific inhibitor; Apo and DPI, NADPH Oxidase inhibitor; NF-κB*i*, NF-κB activation inhibitor; LY83583, cGMP inhibitor; 8-Br-cGMP, cell permeable cGMP analogue; Z-IETD-FMK, caspase-8 inhibitor; KT5823, PKG inhibitor.

We reasoned that movement towards ER led to increased interaction and key to mitochondrial-$Ca^{2+}$ uptake in infected HKM. To prove that, HKM were pre-treated with actin polymerization inhibitor, cyt D[29] and mitochondrial-movement and $Ca^{2+}$ uptake studied. We observed that cyt D interrupted mitochondrial motility towards ER and lowered mitochondrial-$Ca^{2+}$ levels (Fig. 5b, Fig. 5c and Fig. 6a) implicating ER-mitochondria crosstalk critical in the pathogenicity of *A. hydrophila*.

***A. hydrophila*-induced alterations in mitochondrial ultra-structure initiate HKM apoptosis.** Altered mitochondrial architecture is overture to apoptosis[14]. Ultra-structural analysis of *A. hydrophila*-

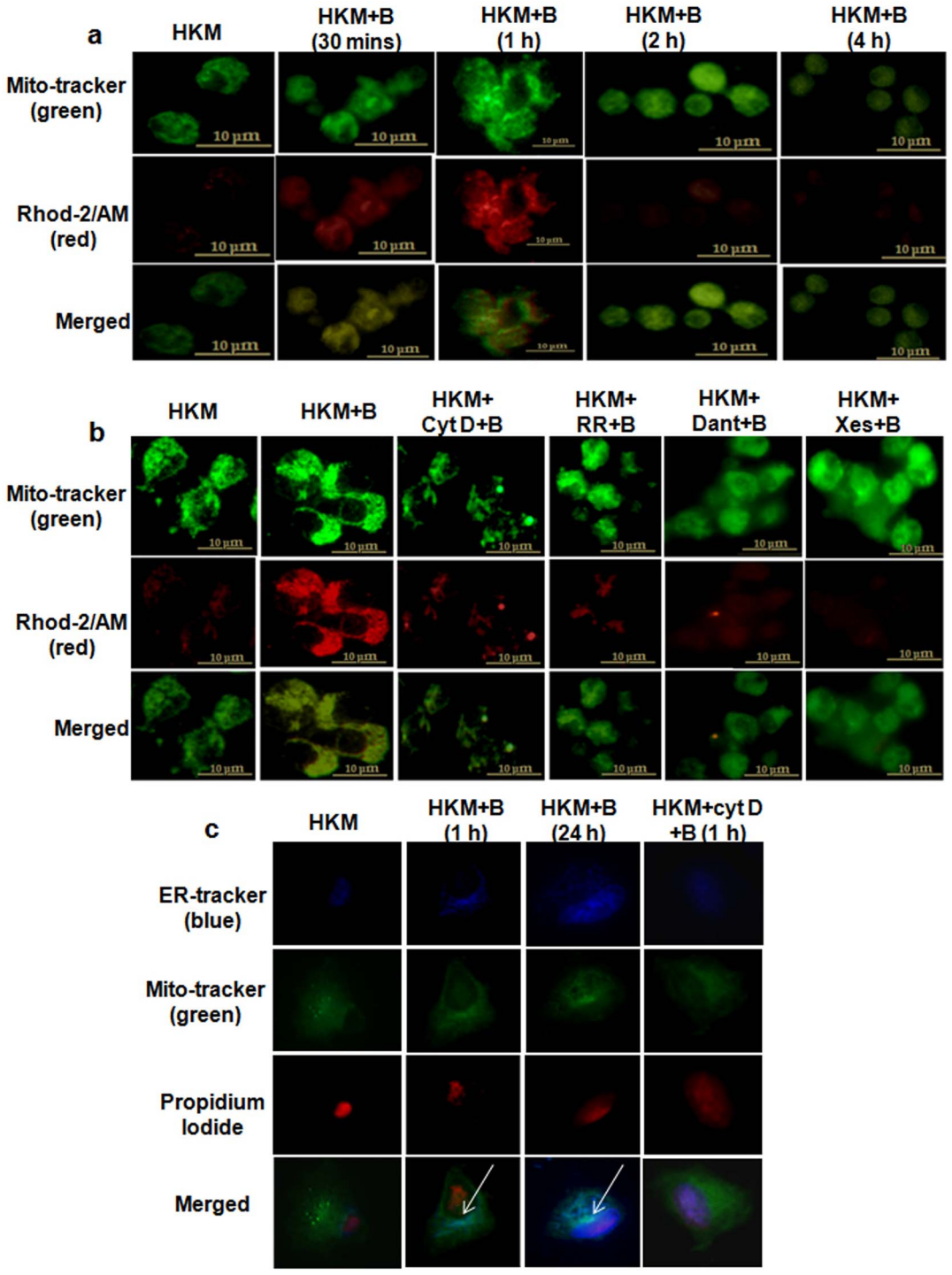


**Figure 5 | $Ca^{2+}$-uptake by mitochondria and its subsequent movement towards ER takes place in *A. hydrophila*-infected HKM.** (a) HKM were infected with *A. hydrophila* and at indicated time point p.i. mitochondrial-$Ca^{2+}$ uptake studied using Rhod-2/AM. (b) HKM were pre-treated separately with cyt D, RR, Xes and Dant and at 1 h p.i. mitochondrial-$Ca^{2+}$ uptake studied using Rhod-2/AM. Mitotracker green is the mitochondrial marker. (c) HKM were infected with *A. hydrophila* and at indicated time p.i., stained with ER tracker (blue), Mitotracker (green) and PI (Propidium iodide, nuclear staining). In another set HKM were pre-treated with cyt D before *A. hydrophila*-infection and at 1 h p.i. ER, mitochondria and nuclear staining were done. The immunofluorescence images are representative of three independent experiments (×100). HKM, uninfected control; HKM + B, HKM infected with *A. hydrophila*; HKM + cyt D + B, HKM pre-treated with cyt D for 1 h before *A. hydrophila*-infection; HKM + RR + B, HKM pre-treated with RR for 1 h before *A. hydrophila*-infection; HKM + Dant + B, HKM pre-treated with dantrolene for 1 h before *A. hydrophila*-infection; HKM + Xes + B, HKM pre-treated with xestospongin C for 1 h before *A. hydrophila*-infection. Cyt D, actin polymerization inhibitor; RR, MUP inhibitor; Xes, IP3R inhibitor; Dant, RyR inhibitor.

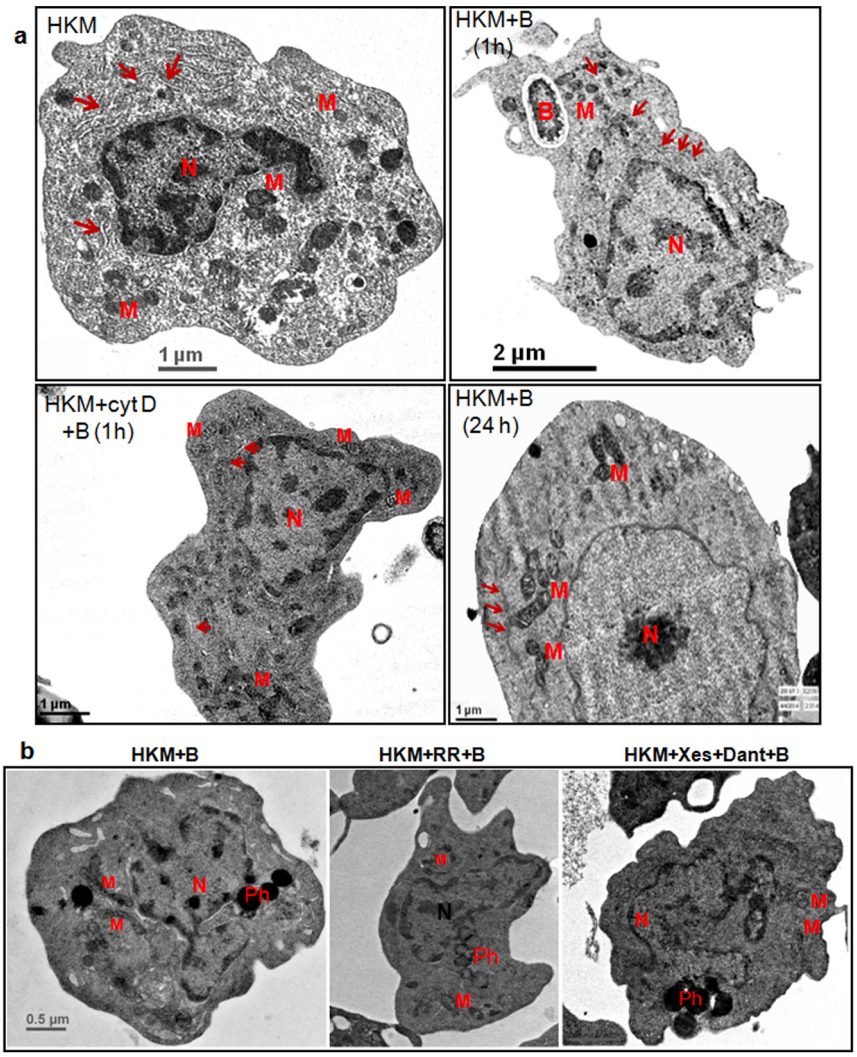


**Figure 6 | $[ER]_{Ca}^{2+}$ uptake alters the mitochondrial ultra-structure in *A. hydrophila*-infected HKM.** (a) HKM were infected with *A. hydrophila* and at indicated time point p.i. mitochondrial positioning with respect to ER studied using TEM. HKM were pre-treated with cyt D and at 1 h p.i. mitochondrial positioning with respect to ER studied using TEM. (b) HKM were pre-treated separately with Dant + Xes and RR and mitochondrial ultra-structural changes studied at 24 h p.i. using TEM. Elongated mitochondria were noted in infected HKM. Arrow indicates ER. Mitochondria, Pseudopodia, Nucleus, Phagosome and Bacteria marked as M, P, N, Ph and B respectively. HKM, uninfected control; HKM + B, HKM infected with *A. hydrophila*; HKM + cyt D + B, HKM pre-treated with cyt D for 1 h before *A. hydrophila*-infection; HKM + Xes + Dant + B, HKM pre-treated together with Xes and Dant for 1 h before *A. hydrophila*-infection; HKM + RR + B, HKM pre-treated with RR for 1 h before *A. hydrophila*-infection. Cyt D, actin polymerization inhibitor; Xes, IP3R inhibitor; Dant, RyR inhibitor; RR, mitochondrial uniporter inhibitor.

infected HKM suggested prominent outlines of mitochondrial cristae as early as 1 h p.i. (Fig. 6a). With the advent of time mitochondria appeared aggregated, more electron-dense, elongated and in direct physical contact around phagosome containing bacteria (Fig. 6a and Supplementary Fig. 4). Besides, the infected HKM were smaller in size, round with retracted pseudopodia and condensed nucleus, characteristic of apoptosing cells.

To check whether $[ER]_{Ca}^{2+}$ depletion was inducing alteration in mitochondrial structure and function, the HKM were pre-treated with Xes and Dant or RR and observed under TEM at 24 h p.i. We observed that Xes and Dant helped in retaining normal mitochondrial ultra-structure (Fig. 6b). We further noted RR pre-treatment restored mitochondrial ultra-structure (Fig. 6b), confirming $Ca^{2+}$-flux through MUP initiate ultra-structural changes in the organelle in *A. hydrophila*-infected HKM.

Alterations in the mitochondrial ultra-structure lead to loss in $\psi_m$[30]. The mitochondrial ultra-structural changes prompted us to study this. The HKM were pre-treated with Xes, Dant or RR prior to *A. hydrophila*-infection and the changes in $\psi_m$ studied using JC-1 at different time p.i. Our confocal microscopic results suggested time dependent reduction of $\psi_m$ in infected HKM (Fig. 7a) which was blocked in the presence of Xes, Dant and RR (Fig. 7b). Mitochondrial-$Ca^{2+}$ overload and $\psi_m$ loss leads to MPTP opening and release of cyt C into cytosol triggering mitochondria-dependent apoptotic cascade[31]. Immunoblotting studies demonstrated cytosolic cyt C release in *A. hydrophila*-infected HKM which was inhibited in presence of CsA, the MPTP inhibitor (Fig. 7c). The $\psi_m$ loss was also prevented in the presence of CsA (Fig. 7b). We concluded that $[ER]_{Ca}^{2+}$-induced mitochondrial dysfunctioning is a key event in *A. hydrophila*-induced HKM apoptosis.

Finally, to prove mitochondrial involvement, we studied caspase-9 activity and recorded significant caspase-9 activation in infected HKM (Fig. 7d). The improved HKM survival (Supplementary Fig. 2) coupled with ameliorated caspase-9 activity in the presence of RR, CsA or Z-LEHD-FMK (Fig. 7d) confirmed that altered mitochondrial dynamics due to $[ER]_{Ca}^{2+}$ depletion led to downstream activa-

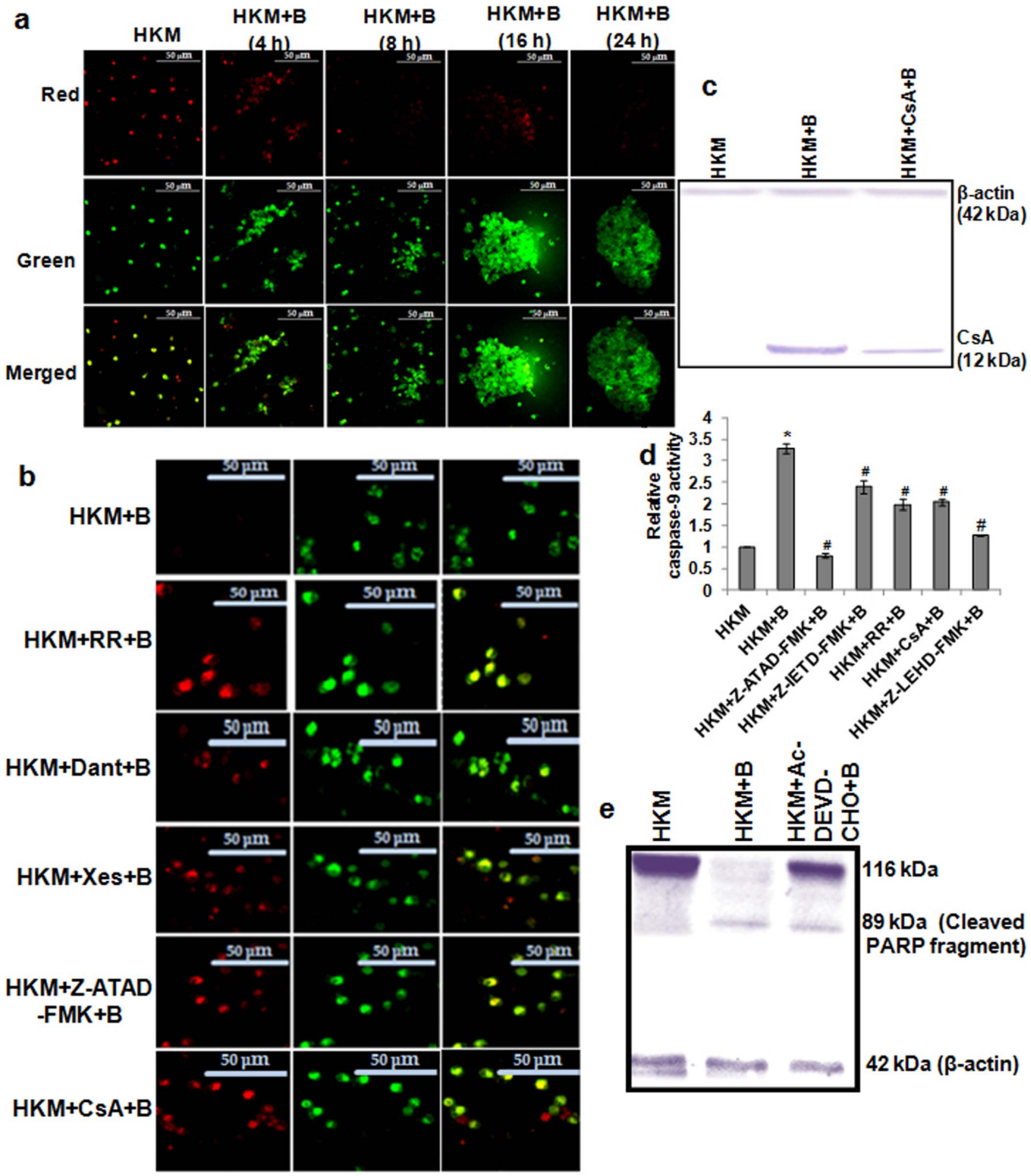


**Figure 7 | Altered $\psi_m$ activates caspase-9 mediated HKM apoptosis.** (a) HKM were infected with *A. hydrophila* and at indicated time p.i. $\Delta\psi_m$ studied using the JC-1 dye. (b) HKM were pre-treated separately with RR, Dant, Xes, CsA, and Z-ATAD-FMK and at 24 h p.i. $\Delta\psi_m$ studied using the JC-1 dye by confocal microscopy (×40). Red images indicate the JC-1 aggregate, while green images indicate JC-1 monomers. Merged images indicate the co-localization of JC-1 aggregates and monomers. (c) Representative western blot of cyt C release in the cytosol in lysates of HKM pre-treated with CsA at 24 h p.i. (d) HKM were pre-treated separately with Z-ATAD-FMK, Z-IETD-FMK, RR, CsA and Z-LEHD-FMK and caspase-9 activity assayed at 24 h p.i. in the lysates. Increase was significant in infected samples relative to uninfected HKM which significantly lowered following pre-incubation with inhibitors (*, $^{\#}P < 0.001/F = 93.65$). (e) Representative western blot of PARP cleavage in lysates of HKM pre-treated with Ac-DEVD-CHO at 24 h p.i. β-actin served as the loading control. The image represents the best of three replicates. **P vs* HKM; $^{\#}P$ *vs* HKM + B. Vertical bars represent mean ± SE (n = 6). HKM, uninfected control; HKM + B, HKM infected with *A. hydrophila*; HKM + Dant + B, HKM pre-treated with dantrolene for 1 h before *A. hydrophila*-infection; HKM + Xes + B, HKM pre-treated with xestospongin C for 1 h before *A. hydrophila*-infection; HKM + RR + B, HKM pre-treated with RR for 1 h before *A. hydrophila*-infection; HKM + Z-ATAD-FMK + B, HKM pre-treated with Z-ATAD-FMK for 1 h before *A. hydrophila*-infection; HKM + CsA + B, HKM pre-treated with CsA for 1 h before *A. hydrophila*-infection; HKM + Z-IETD-FMK + B, HKM pre-treated with Z-IETD-FMK for 1 h before *A. hydrophila*-infection; HKM + Z-LEHD-FMK + B, HKM pre-treated with Z-LEHD-FMK for 1 h before *A. hydrophila*-infection; HKM + Ac-DEVD-CHO + B, HKM pre-treated with Ac-DEVD-CHO for 1 h before *A. hydrophila*-infection. RR, MUP inhibitor; Xes, IP3R inhibitor; Dant, RyR inhibitor; CsA, MPTP inhibitor; Z-ATAD-FMK, caspase-12 inhibitor; Z-IETD-FMK, caspase-8 inhibitor; Z-LEHD-FMK, caspase-9 inhibitor; Ac-DEVD-CHO, caspase-3 inhibitor.

tion of caspase-9 in *A. hydrophila*-infected HKM. In this connection it is important to mention that pre-treatment with caspase-8 inhibitor, Z-IETD-FMK also inhibited caspase-9 activity in infected HKM. This suggests cross-talk between the two caspase pathways initiated by t-Bid[13]. The DNA repair enzyme, PARP is one of the substrates for caspase-3[22]. We noted PARP cleavage in infected HKM which was prevented by caspase-3 inhibitor, Ac-DEVD-CHO (Fig. 7e), further establishing PARP cleavage to be an essential requisite for *A. hydrophila*-induced HKM apoptosis.

## Discussion

*A. hydrophila*-induced macrophage apoptosis is well established[3,4,32,33] although the molecular mechanism remains unknown. The disruption in ER homeostasis in response to various stimuli with pathological implications is reported in fish[34]. However, there are no reports on the role of ER-stress in bacterial-pathogenicity including *A. hydrophila*-infections in fish. Altered $Ca^{2+}$-homeostasis is primal to ER-stress. After observing $Ca^{2+}$ and its dependent molecules critical for *A. hydrophila*-induced HKM apoptosis[4,6] we questioned the involvement of ER-stress in terms of CHOP-BiP-eIF2α-spree and caspase-12 activation.

Elevated expression of CHOP-BiP and phosphorylation of eIF2α were noted. In the absence of fish-specific antibodies we used mammalian antibodies as these proteins show considerable homology, both at nucleotide and protein levels[15]. Among different ER-stress sensors, CHOP plays pro-apoptotic role by modulating the death domain receptor DR5[35]. While eIF2α halts translation of new proteins in ER and is implicated in apoptosis, BiP acts as pro-survival factor under different stress conditions[36]. Earlier reports implicated ER-stress and BiP expression to be critical in betanodavirus-induced apoptosis in fish cells[37]. We wondered the elevated expression of the three ER-stress markers have any correlation with *A. hydrophila*-induced HKM apoptosis. Pre-treatment with the ER-stress inhibitor, 4-PBA inhibited the expression of BiP, CHOP and phospho-eIF2α, restored the normal cyto-architecture (data not shown) and attenuated apoptosis of infected HKM. It is widely perceived that the complex interaction of ER-stress proteins regulates the balance between cell death and survival[38]. We suggest that following infection, the HKM up-regulate BiP for survival but the sustained increase in CHOP and phospho-eIF2α skew the balance in favour of apoptosis. This is the first report suggesting *A. hydrophila* actively induces a UPR that compromises host response. Since, *A. hydrophila* displays wide host specificity it would be interesting to see whether same pathogenic mechanisms are employed across other host species. Microbe-induced ER-stress and UPR has been reported in fish[37] and mammals[36,38–41]. Our study not only extends these findings to *A. hydrophila* but further suggests UPR to be an evolutionarily conserved pathological mechanism.

Earlier studies suggested calpain activation downstream to ER-stress[42]. We observed that 4-PBA attenuated calpain-2 activation in the HKM. Activated calpain-2 is reported to proteolytically activate caspase-12[12]. Importantly, the role of caspase-12 as marker of ER stress-induced apoptosis has been well reported in rodents[43]. The presence and functional significance of caspase-12 in fish has recently been documented[37]. We observed caspase-12 activation to be an obligatory step during *A. hydrophila*-induced HKM apoptosis and calpain-2 playing a role in its activation. The results hence confirmed the ER-stress induced caspase-12 as a novel signalling molecule in *A. hydrophila* pathogenesis.

An inevitable event in apoptosis is mitochondrial dysfunctioning consequent to ER-stress[44]. The Rhod-2 results clearly indicated mitochondrial-$Ca^{2+}$ uptake in *A. hydrophila*-infected HKM. Actin filaments promote the transport of cellular organelles like mitochondria[29,45,46]. Cytochalasin D causes focal aggregation of actin filaments and congestion of cytoplasm causing physical interference with microtubule-based transport and inhibition of mitochondrial movement[29]. We thus used cyt D and our immunofluorescence and TEM studies confirmed the docking of mitochondria and ER in infected HKM which was prevented following cyt D pre-treatment. Besides, cyt D pre-treatment also inhibited mitochondrial-$Ca^{2+}$ uptake implicating mitochondrial motility to be essential for the process. We suspected ER to be the source for mitochondrial-$Ca^{2+}$. Depletion of $[ER]_{Ca^{2+}}$ occurs primarily through IP3R or RyR contributing to apoptosis[47]. We observed that Xes and Dant inhibited ER-stress, uptake of $[ER]_{Ca^{2+}}$ by mitochondria and abrogated apoptosis in infected HKM. Ruthenium Red, an inhibitor of MUP that prevents mitochondrial-$Ca^{2+}$ loading was introduced in the culture[28]. We found that mitochondrial-$Ca^{2+}$ uptake was attenuated in the presence of RR, suggesting MUP-mediated $Ca^{2+}$ uptake inside the organelle. From the results we presume that the docking onto ER promotes more contact sites, ensuring efficient transfer of $[ER]_{Ca^{2+}}$ through MUP leading to apoptotic pathology.

The sequestered $Ca^{2+}$ within mitochondria induces swelling, $\psi_m$ dissipation and release of cyt C into cytosol through MPTP[48]. We observed $[ER]_{Ca^{2+}}$-induced mitochondrial aggregation and ultrastructural changes. We found that the inhibition of $[ER]_{Ca^{2+}}$ release and its uptake by MUP restored HKM morphology. Altered mitochondrial-morphology is a marker of cell's condition[49]. Mitochondrial elongation and aggregation was noted which was also observed during *M. tuberculosis*-induced macrophage apoptosis[50]. In corroboration to earlier findings, we presume from the TEM images that changed mitochondrial structural dynamics accompanies HKM apoptosis. We enquired the impact of mitochondrial-$Ca^{2+}$ uptake and noted $\psi_m$ dissipation. *A. hydrophila*-induced mitochondrial dysfunctioning leading to apoptosis has been reported. However, the underlying molecular mechanisms remain largely unexplained. There are reports suggesting *A. hydrophila*-induced apoptosis resulting from[51] as well as independent of mitochondrial depolarization[3]. We conclude that inhibiting $[ER]_{Ca^{2+}}$ release and its uptake by mitochondria prevents mitochondrial-structural-functional alterations thus implying the ER-mitochondrial interactions in apoptosis of *A. hydrophila*-infected HKM.

Activated caspase-12 induces $\psi_m$ dissipation, the step preceding caspase-9 activation[52]. It was noted that shedding caspase-12 activation restored $\psi_m$ and caspase-9 activity. The results together suggest that ER-stress induced calpain-2 activation followed by caspase-12 activation is critical in *A. hydrophila*-induced HKM pathology.

Our observations established the role of NADPH Oxidase-mediated superoxide ion generation on *A. hydrophila*-induced HKM apoptosis. Interestingly, the role of second messengers on NADPH Oxidase activation in fish or in *A. hydrophila*-pathogenicity was not reported. Hence, we sought to study the role of $Ca^{2+}$-pathway on NADPH Oxidase activation in HKM. The decrease in superoxide ion levels in presence of BAPTA-AM for the first time suggested $Ca^{2+}$-dependency of NADPH Oxidase (data not shown). We reasoned that $Ca^{2+}$ was directly binding and inducing conformational changes necessary for enzyme activity or NADPH Oxidase could be a substrate for $Ca^{2+}$-dependent proteases, like calpains. Indeed, earlier reports suggested a cross-talk between superoxide ion and calpain activation[53,54]. Our results clearly suggest the role of calpain-2 on activating NADPH Oxidase mediated superoxide ion generation in *A. hydrophila*-infected HKM. We also observed that alleviating ER-stress by 4-PBA inhibited superoxide ion generation in the infected HKM (data not shown). We propose that ER-stress is apical to calpain-2 induced superoxide ion generation in *A. hydrophila*-infected HKM.

Coupled to superoxide ion generation is NF-κB activation[23]. We used phospho-p65 as marker for NF-κB activity[24] and results indicated phosphorylation of p65 trans-activation domain on serine 536 and inhibiting p65 phosphorylation and its nuclear translocation attenuated *A. hydrophila*-induced HKM apoptosis. Moreover, p65 phosphorylation and nuclear translocation was inhibited in the pres-

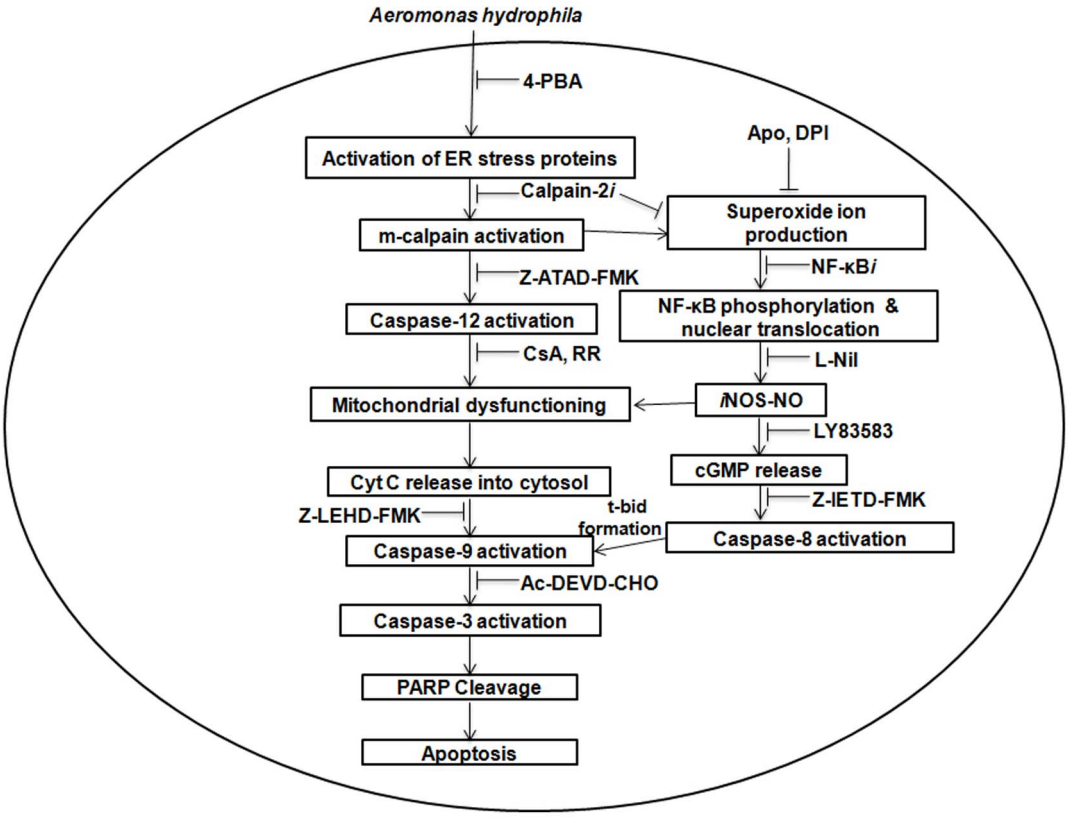


**Figure 8 | Overview of the work.** ER-stress due to $[ER]_{Ca}^{2+}$ depletion activates calpain-2 in the HKM. Calpain-2 plays critical role on the death cascade by activating caspase-12 and superoxide ion-NF-κB axis leading to the release of pro-apoptotic NO which in turn activates the cGMP/PKG pathway. cGMP/PKG activates caspase-8 releasing t-Bid. The uptake of $[ER]_{Ca}^{2+}$ through MUP induces ultra-structural changes in the mitochondria and triggered mitochondria-dependent or caspase-9 mediated apoptotic cascade. The crosstalk between caspase-8 and caspase-9 is instrumental to caspase-3 mediated PARP cleavage and apoptosis of *A. hydrophila*-infected HKM.

ence of superoxide ion inhibitors thus specifying redox-mediated pro-apoptotic NF-κB activation in our model. The results are in line with earlier observations reporting pro-apoptotic involvement of NF-κB in *A. hydrophila*-pathogenicity in mammalian system[3]. ER-stress induces NF-κB activation but the mechanism remains yet to be understood[55]. The observation that 4-PBA inhibits calpain-2-superoxide ion axis together with NF-κB activation being superoxide ion mediated suggests calpain-2 as the link between ER-stress and NF-κB activation in *A. hydrophila*-induced pathogenicity.

A modulatory role of superoxide ion on *i*NOS-induced NO production has been reported with NF-κB as the key intermediate[56]. In corroboration to this we noticed that inhibiting the superoxide ion-NF-κB axis abolished *i*NOS activation and pro-apoptotic NO production. The NO-induced apoptotic signal is principally conveyed by cGMP/PKG pathway[57] and is caspase-8 mediated. We noted that *A. hydrophila*-infection was associated with cGMP production and the amount of cGMP being released is comparable to those recorded during other microbial infections[58] suggesting that such an *A. hydrophila*-induced effect could also be important for the pathogenicity of this bacterium. The inhibition of HKM apoptosis by cGMP-specific inhibitor, LY83583 and its induction following addition of cell permeable cGMP analogue, 8-Br-cGMP proved cGMP to be pro-apoptotic in this system. Alongside, we observed that PKG inhibitor, KT5823 inhibited caspase-8 activation. Truncated-Bid formation in infected HKM was observed and pre-treatment with the caspase-8 inhibitor, Z-IETD-FMK inhibited Bid fragmentation. Caspase-8 activity was also inhibited in presence of NO inhibitor, L-Nil (data not shown); suggesting NO acts *via* cGMP/PKG pathway to trigger caspase-8 activity in *A. hydrophila*-infected HKM. Caspase-8 influences caspase-9 activation *via* t-Bid formation[13]. We observed that Z-IETD-FMK attenuated caspase-9 and thereby caspase-3 activation suggesting t-Bid-mediated crosstalk between extrinsic and intrinsic apoptotic pathways in our model. Together, our results established for the first time the hierarchy of caspase activation culminating in PARP cleavage and apoptosis of *A. hydrophila*-infected fish macrophages.

This study provides new insight into *A. hydrophila*-pathogenicity. We propose that *A. hydrophila*-induced ER-stress leads to calpain-2 mediated activation of caspase-12 and the production of superoxide ion. The redox environment primed NF-κB-*i*NOS/NO axis initiating cGMP/PKG mediated caspase-8 activation. Mitochondrial dysfunctioning due to $[ER]_{Ca}^{2+}$ uptake activated caspase-9. The two initiator caspases crosstalk *via* Bid prompting caspase-3 mediated PARP cleavage and HKM apoptosis (Fig. 8). The ER-mitochondria crosstalk and $Ca^{2+}$ playing a critical role by triggering several downstream effector molecules with implications on apoptotic cascade could be helpful in designing strategies to control *A. hydrophila*-infection and can prove as an effective therapeutic candidate.

## Methods

The chemicals were purchased from Sigma-Aldrich unless mentioned.

**Isolation of HKM.** All experiments were performed according to Animal Ethics Committee [Government of India and University of Delhi (DU/ZOOL/IAEC-R/2013/33)]. Catfish (*Clarias batrachus*) HK suspensions were enriched for phagocytes by adherence following isolation using 34/51% percoll gradient and re-suspended in RPMI-1640 (Gibco) supplemented with 25 mM HEPES, 10% FBS and 1% penicillin-streptomycin (complete-RPMI)[4].

**Bacterial strain and infection studies.** *Aeromonas hydrophila* (strain 500297) was gift from Dr. T. Ramamurthy, NICED, India. The HKM were infected with *A. hydrophila* obtained at late log phase (12 h) with MOI 1 : 50 for 60 mins. The

extracellular bacteria were removed by chloramphenicol (30 μg/mL) and the cells maintained in complete-RPMI[4].

**Apoptosis study.** The HKM were pre-treated with ER-stress alleviator (4-phenyl butyrate, 4-PBA, 10 μM), NADPH Oxidase inhibitor-apocynin (Apo, 100 μM), MPTP formation inhibitor-cyclosporin A (CsA, 5 μM, US Biological), RyR inhibitor-Dantrolene (Dant, 20 μM), *i*NOS-specific inhibitor (L-Nil, 50 μM, Cayman), cGMP inhibitor (LY83583, 20 μM), MUP inhibitor-Ruthenium Red (RR, 20 μM), NF-κB activation inhibitor (NF-κB*i*, 10 nM, Calbiochem), PKG inhibitor (KT5823, 1 μM), IP3R inhibitor-xestospongin C (Xes, 1 μM), Caspase-12 inhibitor (Z-ATAD-FMK, 10 μM, Biovision), Caspase-8 inhibitor (Z-IETD-FMK, 10 μM, Promega), Caspase-9 inhibitor (Z-LEHD-FMK, 10 μM, Calbiochem) for 1 h or flavoenzyme inhibitor-Diphenyleneiodonium (DPI, 10 μM) for 2 h prior to *A. hydrophila*-infection and apoptosis studied at 24 h p.i. using Hoechst 33342 (3.25 μM), AV-FITC-PI (BD-Pharmingen) and caspase-3 assay (Promega). The HKM were stained with Hoechst 33342 or AV-FITC-PI and visualized under fluorescence microscope (Nikon Eclipse 400, ×40)[4]. The caspase-3 assay was done following manufacturer's instructions. Briefly, HKM were collected, re-suspended in lysis buffer, plated with reaction buffer and DEVD-*p*NA, incubated at 30°C for 5 h and absorbance read at 405 nm.

**Superoxide ion and NO generation.** The HKM were infected with *A. hydrophila* and superoxide ion ($O_2^-$) measured using nitroblue tetrazolium (NBT, 1.374 mM) at 0, 1, 2, 4, 8, 12, 16, 24 h p.i. In another set, HKM were pre-treated with Apo, DPI or calpain-2 inhibitor (calpain-2*i*, 50 μM), infected with *A. hydrophila* and $O_2^-$ measured at 4 h p.i. The HKM were infected with *A. hydrophila* and NO generation was measured in culture supernatants at 6, 12, 18, 24 h p.i. using Griess' reagent (Invitrogen-Molecular Probes). In separate experiment, HKM were pre-treated with Apo, DPI, NF-κB*i*, LY83583, L-Nil or KT5823 before *A. hydrophila*-infection and NO generation measured. The amount of nitrite generated was calculated from the $NaNO_2$ standard curve[59].

**Immunofluorescence studies.** The HKM were collected at 1, 2, 4, 8, 16, 24 h p.i., fixed in methanol/acetic acid (1 : 1, v/v) for 30 mins on ice, incubated with blocking and permeabilizing solution (PBS, 2 mg/ml BSA, 0.2 mg/ml saponin). Cells were washed and incubated with primary antibodies for total and phospho-eIF2α (rabbit, 1 : 100, Cell signalling Technology), BiP (rabbit, 1 : 100, Cell signalling Technology) and CHOP (mouse, 1 : 100, Cell signalling Technology) separately overnight at 4°C. The HKM were washed, incubated with TRITC or FITC-conjugated secondary antibody (1 : 200) for 1 h at room temperature (RT) and mounted on microslide with cover slips using fluoroshield. The phospho-p65 (mouse, 1 : 100, Cell signalling Technology) and *i*NOS (mouse, 1 : 250, Abcam) expression were studied similarly at 24 h p.i. Expression of *i*NOS, BiP, CHOP, total and phospho-eIF2α were studied using confocal microscope (×40 oil immersion, 1.30 NA, Nikon Eclipse A1Rsi-T*i*E-300). The corrected total cell fluorescence (CTCF) was analysed by Image J software. Nuclear translocation of phopho-p65 was studied under fluorescence microscope (×100, Nikon Eclipse 400). Nucleus was stained for 15 mins with DAPI (1 μg/ml) before mounting on microslide.

**Enzyme immune assays.** Assays were done as per manufacturer's instruction. For total and phospho-NF-κB activity (Cell signalling Technology), HKM obtained at 30 mins, 1, 4, 8, 16, 24, 36 h p.i. or pre-treated with Apo, DPI, NF-κB*i*, L-Nil before *A. hydrophila*-infection were collected at 24 h p.i., and re-suspended in lysis buffer. The lysates were added into the well of pre-coated microtitre plates, specific detection antibodies added followed by washing and addition of HRP-linked secondary antibody. TMB substrate was added, the reactions terminated and absorbance read at 450 nm. To measure cGMP (Biovision), HKM were pre-treated with LY83583, L-Nil or Z-IETD-FMK before *A. hydrophila*-infection, collected at 24 h p.i., resuspended in 0.1 M HCl and plated. To each well, cGMP antibody was added followed by addition of anti-cGMP-HRP conjugate and incubated at RT. After washing, HRP developer was added, the reaction stopped by adding 1 M HCl and absorbance read at 450 nm.

**Caspase- 8, -9, -12 assays.** The assays are based on spectrophotometric detection of the chromophore-*p*NA after cleavage from the labelled substrate LEHD-*p*NA (caspase-9) and IETD-*p*NA (caspase-8) respectively and done as per manufacturer's instructions (Genescript). For caspase-8 assay, HKM were pre-treated with LY83583, KT5823 or Z-IETD-FMK before *A. hydrophila*-infection. For caspase-9 assay, HKM were pre-treated with Z-ATAD-FMK, Z-IETD-FMK, CsA, RR or Z-LEHD-FMK before *A. hydrophila*-infection. The HKM were collected 24 h p.i., washed, re-suspended in lysis buffer and plated with LEHD-*p*NA and IETD-*p*NA respectively. The plates were incubated at 30°C for 5 h and absorbance read at 405 nm. For caspase-12 assay (Biovision), 1 μl FITC-tagged ATAD-FMK was added to each well and left for 30 mins at 30°C followed by washing in fluorescein wash buffer, mounted and observed under confocal microscope (×40).

**Immunoblotting.** The HKM were collected at 24 h p.i., lysed, equal amount of protein separated by 10% SDS-PAGE and transferred onto PVDF membranes. Membranes were blocked with 1% bovine serum albumin in Tris-buffered saline containing 0.10% Tween-20 (TBST) for 1 h at RT and probed separately with rabbit polyclonal antibodies against calpain-2 (1 : 500, Abcam), Bid (1 : 1000) and PARP (1 : 1000) from Cell Signalling Technology overnight at 4°C. Membranes were incubated for 3 h at RT with AP-conjugated secondary antibody (1 : 1000, Santacruz). Protein loading was normalized by anti-β-actin antibody (rabbit, 1 : 10, 000, Santacruz) followed by incubation with AP-conjugated secondary antibody. For $p47^{phox}$, HKM were collected 4 h p.i., lysed in lysis buffer containing 0.25 M sucrose[60], the cytosolic and membrane-enriched fraction were separated, equal protein then subjected to 10% SDS-PAGE and immunoblotting as mentioned earlier. The membrane fraction was probed with mouse polyclonal antibody against $p47^{phox}$ (1 : 100, Santacruz Biotechnology) and cytosolic fraction was probed with anti-β-actin antibody.

**Mitochondrial-$Ca^{2+}$ imaging.** The HKM obtained at 30 mins, 1, 2 and 4 h p.i. or in sets pre-treated with cyt D, RR, Dant, Xes before *A. hydrophila*-infection were collected at 1 h p.i. Cells were washed and loaded simultaneously with Rhod-2/AM and mitotracker green (Invitrogen-Molecular Probes, 50 nM), incubated at 30°C for 30 mins, again washed, mounted on microslide and observed under fluorescence microscope (×100).

**Mitochondrial membrane potential.** The HKM obtained at 4, 8, 16, 24 h p.i. or in sets pre-treated with RR, Dant, Xes, CsA, Z-ATAD-FMK before *A. hydrophila*-infection were collected at 24 h p.i., washed with PBS and loaded with JC-1 (Invitrogen-Molecular Probes, 20 μM) at 30°C for 15 mins, followed by washing and mounted on microslide. The images were acquired under confocal microscope (×40).

**Cytochrome C detection.** Cytochrome C release was checked using assay kit as per manufacturer's instruction (Biovision). Briefly, HKM pre-treated with CsA before *A. hydrophila*-infection was collected at 24 h p.i. in cytosolic extraction buffer. Cell pellet was homogenized, centrifuged at 700 × *g* for 10 mins at 4°C and the supernatant centrifuged at 10, 000 × *g* for 30 mins at 4°C. The supernatant obtained was collected as cytosolic fraction. The presence of cyt C in cytosolic fraction was checked by immunoblotting using mouse cyt C antibody (1 μg/mL) as mentioned earlier. Equal loading was confirmed by β-actin.

**Mitochondrial and ER network imaging.** The HKM obtained at 1 and 24 h p.i. or in set pre-treated with cyt D before *A. hydrophila*-infection were collected at 1 h p.i. Cells were washed with PBS, loaded with ER-tracker and mitotracker green (Invitrogen-Molecular Probes, 10 nM) for ER and mitochondrial imaging respectively at 30°C for 15 mins and mounted on microslide. The images were acquired under fluorescence microscope (×100).

**TEM analysis.** The HKM obtained at 1 and 24 h p.i. or in sets pre-treated with cyt D, RR or Xes + Dant before *A. hydrophila*-infection were collected, washed in 0.1 M phosphate buffer and incubated with 2.5% glutraldehyde at 4°C for 8 h. Unreacted glutaraldehyde was removed by washing, resuspended in 1% OsO4, incubated for 2 h and again washed. Dehydration was done in ethanol gradient followed by changes in 100% propylene oxide. Samples were embedded in Araldite resin (CY212) and blocks polymerized at 60°C for 48 h. Ultra-thin sections (60–80 nm) were cut (Leica Ultracut 6), stained with uranyl acetate (BDH)-lead citrate (Polaron) and grids examined at 80 kV in TEM (FEI, Morgagni, 268D).

**Statistical analysis.** Mean ± SE were calculated and statistical analysis was performed by one way ANOVA followed by Newman-Keuls *post hoc* test.


1. Janda, J. M. & Abbott, S. L. The genus *Aeromonas*: Taxonomy, pathogenicity and infection. *Clin. Microbiol. Rev.* **23**, 35–73 (2010).
2. Suarez, G. *et al.* A type VI secretion system effector protein, VgrG1, from *Aeromonas hydrophila* that induces host cell toxicity by ADP ribosylation of actin. *J. Bacteriol.* **192**, 155–168 (2010).
3. Galindo, C. L. *et al. Aeromonas hydrophila* cytotoxic enterotoxin activates mitogen-activated protein kinases and induces apoptosis in murine macrophages and human intestinal epithelial cells. *J. Biol. Chem.* **279**, 37597–37612 (2004).
4. Banerjee, C., Goswami, R., Verma, G., Datta, M. & Mazumder, S. *Aeromonas hydrophila* induced head kidney macrophage apoptosis in *Clarias batrachus* involves the activation of calpain and is caspase-3 mediated. *Dev. Comp. Immunol.* **37**, 323–333 (2012).
5. Ashida, H. *et al.* Cell death and infection: A double-edged sword for host and pathogen survival. *J. Cell Biol.* **195**, 931–942 (2011).
6. Banerjee, C., Khatri, P., Raman, R., Bhatia, H., Datta, M. & Mazumder, S. Role of calmodulin-calmodulin Kinase II, cAMP/protein kinase A and ERK 1/2 on *Aeromonas hydrophila*-induced apoptosis of head kidney macrophages. *PLoS Pathog.* **doi:10.1371/journal.ppat.1004018** (2014).
7. Nicotera, P. & Orrenius, S. The role of calcium in apoptosis. *Cell Calcium* **23**, 173–180 (1998).
8. Yamamoto, Y. & Gaynor, R. B. Role of the NF-κB pathway in the pathogenesis of human disease states. *Curr. Mol. Med.* **1**, 287–296 (2001).
9. Forstermann, U. & Sessa, W. C. Nitric oxide synthases: regulation and function. *Eur. Heart J.* **33**, 829–837 (2011).
10. Chami, M. *et al.* Role of SERCA1 truncated isoform in the pro-apoptotic calcium transfer from ER to mitochondria during ER stress. *Cell* **32**, 641–651 (2008).
11. Malhotra, J. D. & Kaufman, R. J. ER stress and its functional link to mitochondria: role in cell survival and death. *Cold Spring Harb. Perspect. Biol.* **doi:10.1101/cshperspect.a004424** (2011).
12. Nakagawa, T. & Yuan, J. Cross-talk between two cysteine protease families: activation of caspase-12 by calpain in apoptosis. *J. Cell Biol.* **150**, 887–894 (2000).
13. Schug, Z. T., Gonzalvez, Z. T., Houtkooper, R. H., Vaz, F. M. & Gottlieb, E. BID is cleaved by caspase-8 within a native complex on the mitochondrial membrane. *Cell Death Diff.* **18**, 538–548 (2011).

14. Rizzuto, R. & Pozzan, T. Microdomains of intracellular $Ca^{2+}$: Molecular determinants and functional consequences. *Physiol. Rev.* **86**, 369–408 (2006).
15. Ishikawa, T., Taniguchi, Y., Okada, T., Takeda, S. & Mori, K. Vertebrate unfolded protein response: mammalian signaling pathways are conserved in medaka fish. *Cell Struct. Funct.* **36**, 247–259 (2011).
16. Magor, B. G. & Magor, K. E. Evolution of effectors and receptors of innate immunity. *Dev. Comp. Immunol.* **25**, 651–682 (2001).
17. MacKenzie, S. *et al.* Comparative analysis of the acute response of the trout, *O. mykiss*, head kidney to *in vivo* challenge with virulent and attenuated infectious hematopoietic necrosis virus and LPS-induced inflammation. *BMC Genomics* **doi:10.1186/1471-2164-9-141** (2008).
18. Majumdar, T., Ghosh, S., Pal, J. & Mazumder, S. Possible role of a plasmid in the pathogenesis of a fish disease caused by *Aeromonas hydrophila*. *Aquaculture* **256**, 95–104 (2006).
19. Shao, J. Z., Liu, J. & Xiang, L. *Aeromonas hydrophila* induces apoptosis in *Carassius auratus* lymphocytes *in vitro*. *Aquaculture* **229**, 11–23 (2004).
20. Mekahli, D., Bultynck, G., Parys, J. B. & de Smedt, H. M. L. Endoplasmic-reticulum calcium depletion and disease. *Cold Spring Harb. Perspect. Biol.* **doi: 10.1101/cshperspect.a004317** (2011).
21. Grayfer, L., Hodgkinson, J. W. & Belosevic, M. Antimicrobial responses of teleost phagocytes and innate immune evasion strategies of intracellular bacteria. *Dev. Comp. Immunol.* **43**, 223–242 (2014).
22. Datta, S., Mazumder, S., Ghosh, D., Dey, S. & Bhattacharya, S. Low concentration of arsenic could induce caspase-3 mediated head kidney macrophage apoptosis with JNK-p38 activation in *Clarias batrachus*. *Toxicol. Appl. Pharmacol.* **241**, 329–338 (2009).
23. Kabe, Y., Ando, K., Hirao, S., Yoshida, M. & Handa, H. Redox regulation of NF-kappaB activation: distinct redox regulation between the cytoplasm and the nucleus. *Antioxid. Redox Signal.* **7**, 395–403 (2005).
24. Chaturvedi, M. M., Sung, B., Yadav, V. R., Kannappan, R. & Aggarwal, B. B. NF-κB addiction and its role in cancer: 'one size does not fit all'. *Oncogene* **30**, 1615–1630 (2011).
25. Saeij, J. P. J. *et al.* Molecular and functional characterization of a fish inducible-type nitric oxide synthase. *Immunogenetic* **51**, 339–346 (2000).
26. Ota, K. T. The NO-cGMP-PKG signaling pathway regulates synaptic plasticity and fear memory consolidation in the lateral amygdala *via* activation of ERK/MAP kinase. *Learn. Mem.* **15**, 792–805 (2008).
27. Yang, B. & Bouchard, M. J. The hepatitis b virus x protein elevates cytosolic calcium signals by modulating mitochondrial calcium uptake. *J. Virol.* **86**, 313–327 (2012).
28. De Stefani, D., Raffaello, A., Teardo, E., Szabo, I. & Rizzuto, R. A forty-kilodalton protein of the inner membrane is the mitochondrial calcium uniporter. *Nature* **476**, 336–340 (2011).
29. Ligon, L. A. & Steward, O. Role of microtubules and actin filaments in the movement of mitochondria in the axons and dendrites of cultured hippocampal neurons. *J. Comp. Neurol.* **427**, 351–361 (2000).
30. Seo, A. Y. New insights into the role of mitochondria in aging: mitochondrial dynamics and more. *J. Cell Sci.* **123**, 2533–2542 (2008).
31. Jacobson, J. & Duchen, M. R. Mitochondrial oxidative stress and cell death in astrocytes requirement for stored $Ca^{2+}$ and sustained opening of the permeability transition pore. *J. Cell Sci.* **115**, 1175–1188 (2002).
32. Ribardo, D. A. *et al.* Early cell signaling by the cytotoxic enterotoxin of *Aeromonas hydrophila* in macrophages. *Microb. Pathog.* **32**, 149–163 (2002).
33. Galindo, C. L. *et al.* Identification of *Aeromonas hydrophila* cytotoxic enterotoxin-induced genes in macrophages using microarrays. *J. Biol. Chem.* **278**, 40198–40212 (2003).
34. Thakur, P. C., Davison, P. C., Stuckenholz, C., Lu, L. & Bahary, N. Dysregulated phosphatidylinositol signaling promotes endoplasmic-reticulum-stress-mediated intestinal mucosal injury and inflammation in zebrafish. *Dis. Model Mech.* **7**, 93–106 (2014).
35. Yamaguchi, H. & Wang, H. G. CHOP is involved in endoplasmic reticulum stress-induced apoptosis by enhancing DR5 expression in human carcinoma cells. *J. Biol. Chem.* **279**, 45495–45502 (2004).
36. Lim, Y. J. Endoplasmic reticulum stress pathway-mediated apoptosis in macrophages contributes to the survival of *Mycobacterium tuberculosis*. *PLoS One* **doi:10.1371/journal.pone.0028531** (2011).
37. Su, Y. C., Wu, J. L. & Hong, J. R. Betanodavirus up-regulates chaperone GRP78 *via* ER stress: roles of GRP78 in viral replication and host mitochondria-mediated cell death. *Apoptosis* **16**, 272–287 (2011).
38. Pillich, H., Loose, M., Zimmer, K. P. & Chakraborty, T. Activation of the unfolded protein response by *Listeria monocytogenes*. *Cell. Microbiol.* **14**, 949–964 (2012).
39. Rolhion, N. *et al.* Abnormally expressed ER stress response chaperone Gp96 in CD favours adherent-invasive *Escherichia coli* invasion. *Gut* **59**, 1355–1362 (2010).
40. Lee, S. Y., Lee, M. S., Cherla, R. P. & Tesh, V. L. Shiga toxin 1 induces apoptosis through the endoplasmic reticulum stress response in human monocytic cells. *Cell. Microbiol.* **10**, 770–780 (2008).
41. Goodall, J. C. *et al.* Endoplasmic reticulum stress-induced transcription factor, CHOP, is crucial for dendritic cell IL-23 expression. *Proc. Nat. Acad. Sci.USA* **107**, 17698–17703 (2010).
42. Tabas, I. & Ron, D. Integrating the mechanisms of apoptosis induced by endoplasmic reticulum stress. *Nat. Cell Biol.* **13**, 184–190 (2011).
43. Martinon, F. & Tschopp, J. Inflammatory caspases: Linking an intracellular innate immune system to autoinflammatory diseases. *Cell* **117**, 561–574 (2004).
44. Kornmann, B., Osman, C. & Walter, P. The conserved GTPase Gem1 regulates endoplasmic reticulum-mitochondria connections. *Proc. Nat. Acad. Sci.USA* **108**, 14151–14156 (2011).
45. Goode, B. L., Drubin, D. G. & Barnes, G. Functional cooperation between the microtubule and actin cytoskeletons. *Curr. Opin. Cell Biol.* **12**, 63–71 (2000).
46. Bravo, R. *et al.* Increased ER-mitochondrial coupling promotes mitochondrial respiration and bioenergetics during early phases of ER stress. *J. Cell Sci.* **124**, 2143–2152 (2011).
47. Luciani, D. S. *et al.* Roles of IP3R and RyR $Ca^{2+}$ channels in endoplasmic reticulum stress and cell death. *Diabetes* **58**, 422–432 (2009).
48. Jeong, S. Y. & Seol, D. W. The role of mitochondria in apoptosis. *BMB Rep.* **41**, 11–22 (2008).
49. Rambold, A. S., Kostelecky, B., Elia, N. & Schwartz, J. L. Tubular network formation protects mitochondria from autophagosomal degradation during nutrient starvation. *Proc. Nat. Acad. Sci. USA* **108**, 10190–10195 (2011).
50. Jamwal, S. *et al.* Characterizing virulence-specific perturbations in the mitochondrial function of macrophages infected with *Mycobacterium tuberculosis*. *Sc. Rep.* **doi: 10.1038/srep01328** (2013).
51. Krzyminska, S. *et al.* *Aeromonas* spp. induce apoptosis of epithelial cells through an oxidant-dependent activation of the mitochondrial pathway. *J. Med. Microbiol.* **60**, 889–898 (2011).
52. Rao, R. V. *et al.* Coupling endoplasmic reticulum stress to the cell death program. An Apaf-1-independent intrinsic pathway. *J. Biol. Chem.* **277**, 21836–21842 (2002).
53. Jeong, J. C. *et al.* Silibinin induces apoptosis *via* calpain-dependent AIF nuclear translocation in U87MG human glioma cell death. *J. Exp. Clin. Cancer Res.* **doi:10. 1186/1756-9966-30-44** (2011).
54. Sobhan, P. K. *et al.* Calpain and reactive oxygen species targets bax for mitochondrial permeabilisation and caspase activation in zerumbone induced apoptosis. *PLoS One* **doi: 10.1371/journal.pone.0059350** (2013).
55. Tam, A. B., Mercado, E. L., Hoffmann, A. & Niwa, M. ER stress activates NF-κB by integrating functions of basal IKK Activity, IRE1 and PERK. *PLoS One.* **doi: 10.1371/journal.pone.0045078** (2012).
56. Mendes, A. F. *et al.* Role of nitric oxide in the activation of NF-κB, AP-1 and NOS II expression in articular chondrocytes. *Nitric Oxide: Biol. Ch.* **6**, 35–44 (2002).
57. Choi, B. M. *et al.* Nitric Oxide as a pro-apoptotic as well as anti-apoptotic modulator. *J. Biochem. Mol. Biol.* **35**, 116–126 (2002).
58. Mittal, R. & Prasadarao, N. V. Nitric oxide/cGMP signalling induces *Escherichia coli* K1 receptor expression and modulates the permeability in human brain endothelial cell monolayers during invasion. *Cell. Microbiol.* **12**, 67–83 (2010).
59. Banerjee, C., Singh, A., Raman, R. & Mazumder, S. Calmodulin-CaMKII mediated alteration of oxidative stress: Interplay of cAMP/PKA-ERK 1/2-NF-κB-NO axis on arsenic induced head kidney macrophage apoptosis. *Tox. Res.* **2**, 413–426 (2013).
60. Plummer, D. T. [Cell Fractionation] *Introduction to Practical Biochemistry* [265–269] (Tata Mc-Graw-Hill, New Delhi, 1988).


## Acknowledgments

This work was supported by DBT grant, BT/PR13883/AAQ/03/516/2010 and University of Delhi Doctoral Research Programme, Dean (R)/R&D/2012/917. We would like to acknowledge A. Pal for technical assistance. The authors are grateful to S. Das, North Shore University Health System and T. Majumdar, Cleveland State University for helpful discussions and critically analyzing the manuscript. The authors are also grateful to M. Shakarad, University of Delhi for his help with statistical analysis. C.B. and A.S. (Ambika) was supported by fellowships from DST-INSPIRE (Govt. of India) and UGC (Govt. of India) respectively.

## Author contributions

C.B. performed the experiments, analysed the data and wrote the paper. A.S. (Ambika) performed the experiments. T.G. performed the experiments and analysed the data. A.S. and R.R. analysed the data. S.M. analysed the data and wrote the paper.

## Additional information

**Supplementary information** accompanies this paper at http://www.nature.com/scientificreports

**Competing financial interests:** The authors declare no competing financial interests.

**How to cite this article:** Banerjee, C. *et al.* Ameliorating ER-stress attenuates *Aeromonas hydrophila*-induced mitochondrial dysfunctioning and caspase mediated HKM apoptosis in *Clarias batrachus*. *Sci. Rep.* **4**, 5820; DOI:10.1038/srep05820 (2014).